Plant Biotechnology Persa

Ilam University of Medical Sciences

Online ISSN: 2676-7414

Homepage: https://pbp.medilam.ac.ir

Development and Evaluation of a Novel DPP-4 Targeted Multi-Epitope Vaccine for Diabetes Mellitus Management: A Comprehensive Immunoinformatic Approach

Farnoush Abdi [1]✉, **Sako Mirzaie**[2]

[1] Institute of Medical Science, University of Toronto, Canada

[2] Department of Pharmaceutical Sciences, Leslie Dan Faculty of Pharmacy, University of Toronto, Toronto, Canada

Article Info

Article type:
Review Article

Article History:
Received: 03 Aug 2025
Revised: 14 Oct 2025
Accepted: 16 Oct 2025
Published Online: 16 Nov 2025

✉ ***Correspondence to:***
farnoush Abdi

Email:
f.abdi@mail.utoronto.ca

A B S T R A C T

Objective: Diabetes mellitus (DM) is a chronic metabolic disorder with a rapidly increasing global prevalence, posing serious health and economic challenges. Current pharmacological treatments often require lifelong administration and may lead to adverse effects or poor patient compliance. This study aimed to design and evaluate a novel peptide-based vaccine targeting the dipeptidyl peptidase-4 (DPP-4) enzyme as an innovative immunotherapeutic approach for the management of diabetes mellitus.

Methods: A multi-epitope vaccine was constructed by combining six cytotoxic T lymphocyte (CTL) epitopes and one helper T lymphocyte (HTL) epitope, integrated with an immunogenic adjuvant sequence. Comprehensive bioinformatics analyses were employed to predict antigenicity, allergenicity, physicochemical characteristics, and structural stability. Molecular docking and molecular dynamics simulations were used to assess vaccine binding affinity and interaction stability with Toll-like receptor 4 (TLR4). Furthermore, in silico immune simulations were conducted to evaluate the predicted immune response.

Results: The designed vaccine exhibited high antigenicity, non-allergenic properties, and favorable physicochemical stability. Docking and dynamics results revealed a strong and stable interaction between the vaccine construct and TLR4. Immune simulations predicted significant activation of both humoral and cell-mediated immune responses.

Conclusion: The proposed DPP-4-targeted peptide vaccine demonstrates strong potential as a novel immunotherapeutic strategy for diabetes mellitus. It could serve as an alternative to conventional treatments by reducing lifelong drug dependency, improving patient adherence, and alleviating the economic burden of the disease.

Keywords: Diabetes mellitus; glucagon-like peptide-1; peptide vaccine; Toll-like receptor 4; dipeptidyl peptidase-4

➢ **How to cite this paper**

Abdi F, Mirzaei S. Development and Evaluation of a Novel DPP-4 Targeted Multi-Epitope Vaccine for Diabetes Mellitus Management: A Comprehensive Immunoinformatic Approach. Plant Biotechnology Persa. 2026; 8(2): Proof.

DOI:
Publisher: Ilam University of Medical Sciences

Introduction

Diabetes mellitus (DM) has become a significant global health challenge, with over two million new cases diagnosed worldwide in the last thirty years, affecting populations across all regions [1]. Type 2 diabetes mellitus (T2DM) is primarily characterized by chronic hyperglycemia resulting from insulin resistance, whereas type 1 diabetes mellitus (T1DM) involves autoimmune destruction of pancreatic β-cells responsible for insulin secretion [1]. Current estimates suggest that by 2030, more than 500 million individuals globally will be living with diabetes, a substantial increase from the current figure of approximately 300 million [2]. In the United States alone, the Centers for Disease Control and Prevention (CDC) reported that in 2010, about 25.8 million people, representing 7.8% of the population, were diagnosed with diabetes [3]. The rising prevalence of DM poses a serious threat to public health worldwide, as it is associated with a growing burden of complications and mortality [4]. Symptoms of diabetes can affect many different systems, including the micro-systems of the retina, the nephrons, and the nervous system, as well as the macrosystems of the heart, the arteries, and peripheral tissue, microvascular complications include stroke, coronary artery disease, cerebral vascular disease, and diabetic foot, resulting in amputations [5]. Effective management of DM aims to prevent or delay these long-term complications by maintaining optimal glucose control. However, this remains challenging due to the progressive nature of the disease, often necessitating treatment intensification and insulin therapy in many patients [6]. Under hyperglycemic conditions, glucagon-like peptide-1 (GLP-1), inhibits glucagon secretion, and improves hyperglycemia [6]. There is a very low inherent risk of hypoglycemia due to the GLP-1–mediated dependent stimulation of insulin secretion. Dipeptidyl peptidase IV (DPP-4) is an enzyme responsible for the rapid degradation of GLP-1, thereby limiting its biological activity and half-life. Also known as CD26, DPP-4 is a multifunctional enzyme expressed on lymphocyte surfaces and in soluble form in the circulation, where it participates in intracellular signaling via its short intracellular tail [7]. Pharmacological inhibition of DPP-4 has become a widely accepted therapeutic approach for T2DM, often used as a second-line treatment after metformin failure. Fixed-dose combinations of metformin and DPP-4 inhibitors have been developed to improve glycemic control and patient compliance. In cases where metformin is contraindicated or not tolerated, DPP-4 inhibitors may be prescribed as monotherapy [8]. Sitagliptin, introduced in 2006, was the first DPP-4 inhibitor approved, followed by others such as linagliptin, vildagliptin, saxagliptin, and alogliptin, which are some of the most widely used medicines. Despite their efficacy, the success of DPP-4 inhibitors is sometimes limited by inconsistent medication adherence and the economic burden associated with lifelong treatment. These challenges have motivated the exploration of novel immunotherapeutic strategies aimed at improving treatment outcomes and patient compliance in diabetes management [9]. However, there are some limitations to the success of treatment due to inconsistent drug intake and the significant economic burden that is associated with lifelong treatment. A novel immunotherapeutic method has been developed and tested for the treatment of T2DM in order to address adherence challenges and enhance treatment efficacy for patients [10]. On the other hand, it has been shown that vaccines are an effective method of preventing infectious diseases, as well as for managing chronic conditions such as hypertension and Alzheimer's disease [11]. The sustained effects of vaccines and the lack of a daily dose requirement make vaccination an attractive alternative to conventional therapy at a low cost [12]. One method of preventing or reversing diabetes development is by protecting, replacing, or regenerating cells. As insights into the autoimmune mechanisms underlying diabetes have advanced, there has been growing interest in the potential application of immunomodulatory agents often termed vaccines to prevent or better regulate DM. Studies have shown that immunosuppressive treatments with agents like cyclosporin, azathioprine, or cyclophosphamide can temporarily reduce insulin dependency in T1DM, indicating that modulating the immune response can improve disease outcomes. Vaccines can alter the immune system in multiple ways, including shifting from a harmful (e.g., Th1) to a more tolerogenic (e.g., Th2) response, inducing antigen-specific regulatory T cells, eliminating autoreactive T cells, or disrupting immune cell interactions [13,14]. The development of various immunoinformatic tools paved a walkway for vaccine design and caused time and money saving. Several

software platforms and databases enable the analysis of genetic information from target proteins to identify promising vaccine candidates. Numerous studies have employed immunoinformatic methodologies to develop vaccines targeting pathogenic viruses, bacteria, and parasites [15,16]. In this work, we aimed to design a novel multi-epitope mRNA vaccine based on DPP-4, incorporating a potent immunogenic adjuvant and other essential components using an immunoinformatic approach.

Materials and methods

Retrieval of DPP-4 sequence

The reference amino acid sequence of the human DPP-4 protein, identified by the accession number P27487, was obtained from the UniProt database (https://www.uniprot.org/uniprotkb/P27487/entry).

Identifying and selecting epitopes for T-cells

Before any specific study, we used the full length of DPP-4 to check if it is an Antigen. After confirming, the further studies were conducted. Cytotoxic T lymphocyte (CTL) epitopes within DPP-4 were predicted using the NetCTL 1.2 server (https://services.healthtech.dtu.dk/service.php?NetCTL-1.2) (18). This tool predicts 9-mer CTL epitopes restricted to 12 MHC class I supertypes, including A1, A2, A3, A24, A26, B7, B8, B27, B39, B44, B58, and B62. The studies were conducted using three approaches: proteasomal cleavage of the C-terminus, Transporter associated with Antigen Presentation (TAP) transport efficiency, and the prediction including the binding affinity of MHC class-I molecules. TAP transport efficiency was assessed using a weight matrix, while artificial neural networks were employed to predict MHC-I binding and proteasomal cleavage. A threshold score of 0.75 was applied to select potential epitopes. Helper T lymphocyte (HTL) epitopes were identified using the NetMHCII 2.3 server (https://services.healthtech.dtu.dk/service.php?NetMHCII-2.3) (Oli, 2020), which utilizes artificial neural networks to predict binding of 15-mer peptides to HLA-DR, HLA-DQ, HLA-DP, and murine MHC class II alleles. Binding thresholds of 2% and 10% were set to classify strong and weak binders, respectively. To refine epitope selection, candidates were further evaluated for antigenicity, toxicity, and allergenicity. Antigenicity predictions were performed using the VaxiJen v2.0 server (https://www.ddg-pharmfac.net/vaxijen/VaxiJen/VaxiJen.html). It has been found that the accuracy of the prediction by this server is between 70 to 89%. The ToxinPred server [17] employing an SVM-based model trained on Swiss-Prot data. Allergenicity was evaluated using AllerTOP version 2.0 (https://www.ddg-pharmfac.net/AllerTOP/index.html). The selected epitopes formed the basis for constructing a multi-epitope vaccine. To ensure proper spacing and presentation of CTL epitopes, AAY linkers were incorporated. These linkers facilitate a more organized presentation of the epitopes. Furthermore, the 50S ribosomal protein L7/L12 (Locus RL7_MYCTU), accession number P9WHE3, was included as an adjuvant to enhance immunogenicity. Its amino acid sequence was fused to the N-terminal region of the construct using an EAAAK linker to maintain structural integrity.

In silico analysis of antigenic potential, allergenic risk, and physicochemical features of the vaccine

Assessing the antigenic properties is a vital step in the vaccine development procedure. We employed two tools, VaxiJen v2.0 and ANTIGENpro, to predict the antigenic characteristics of the ultimate vaccine structure. ANTIGENpro (available at http://scratch.proteomics.ics.uci.edu/) uses five machine learning techniques and diverse forms of the primary sequence were utilized to predict protein antigenicity [18]. Furthermore, we utilized the ExPASy ProtParam server (available at https://web.expasy.org/protparam/) to analyze the physicochemical properties of the constructed vaccine candidate. The evaluated parameters included amino acid composition, molecular weight, theoretical isoelectric point (pI), instability index, estimated half-life, aliphatic index, and the grand average of hydropathicity (GRAVY) [19].

Prediction of secondary structure of vaccine construct

The Prabi server (accessible at https://npsa-prabi.ibcp.fr/cgi-bin/npsa_automat.pl?page=/NPSA/npsa_gor4.html) was utilized to estimate the proportion of secondary structure components in the designed vaccine construct. This server employs the GOR IV prediction method, known for its average accuracy rate of 64.4% [20].

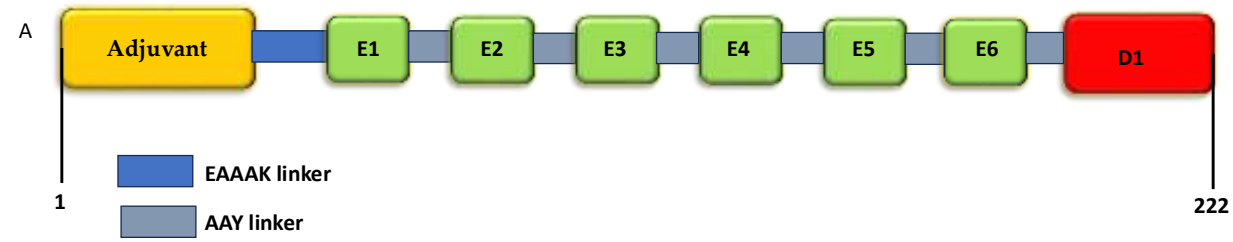

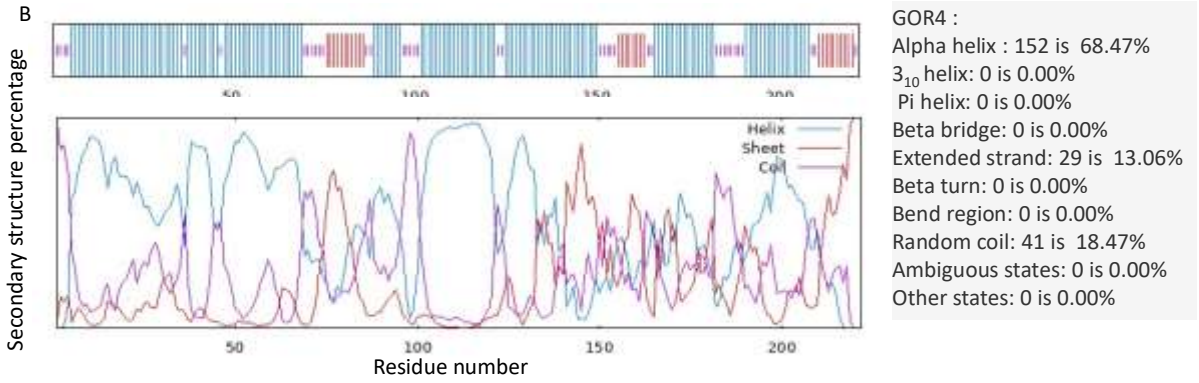

GOR4 :

Alpha helix : 152 is 68.47%

310 helix: 0 is 0.00%

Pi helix: 0 is 0.00%

Beta bridge: 0 is 0.00%

Extended strand: 29 is 13.06%

Beta turn: 0 is 0.00%

Bend region: 0 is 0.00%

Random coil: 41 is 18.47%

Ambiguous states: 0 is 0.00%

Other states: 0 is 0.00%

Model generation, refining, and validating the three-dimensional structure of the multi-epitope protein structure.

The I-TASSER server (accessible at https://zhanglab.ccmb.med.umich.edu/I-TASSER/) was employed to predict the three-dimensional structure of the multi-epitope vaccine. This server computationally predicts three-dimensional structures based on the amino acid sequence, assembling fragments from threading templates and provides a C-score to evaluate the accuracy of the generated models [21]. The quality of the models was measured by using ProTSAV server [22]. This server is a thoroughly validated server, having undergone testing on a dataset comprising around 64,446 protein structures. This dataset includes a diverse set of structures, such as obtained experimentally from RCSB and structures from publicly available decoy sets. When applied to experimentally determined frameworks, ProTSAV demonstrates an achieved

100% specificity with 98% sensitivity. In the case of estimated protein structural models for CASP11 targets with resolutions at below 2 Å resolution, the method reached 88% specificity and 91% sensitivity. By combining various approaches, this server effectively overcomes the limitations associated with standalone servers or techniques, establishing itself as a reliable platform for evaluating quality [22]. The chosen model was further refined using the GalaxyRefine2 web server [23].

In silico prediction of B-cell epitopes

B-lymphocytes play a central role in the immune system, being responsible for antibody production, which in turn supports the induction of durable immunity [24]. The prediction of linear B-cell epitopes was conducted using the BCPREDS server, accessible at https://webs.iiitd.edu.in/raghava/bcepred/bcepred_submission.html [25]. This server utilizes a subsequence kernel-based SVM classifier and demonstrates a 74.57% accuracy rate in the prediction of linear B-cell epitopes [26]. Additionally, for the prediction of discontinuous B-cell epitopes, we utilized the ElliPro server, available at http://tools.iedb.org/ellipro/ [27]. ElliPro utilizes residue-based clustering together with Thornton's method to predict epitopes, assigning each one a protrusion index (PI) score.

Molecular docking and molecular dynamics (MD) simulation

The CTL and HTL epitopes that met the screening criteria were further analyzed through molecular docking with MHC class I molecules (A1, A2, A3, A26, and B58) and MHC class II (DRB1). HyperChem 8 facilitated the construction of the epitope structures [28]. Autodock vina [29] operated with its default parameters, was employed to dock the epitopes with MHC molecules. Following epitope assembly, adjuvant incorporation, and vaccine construct design, a 500 ns molecular dynamics (MD) simulation was performed to refine the structure and resolve steric hindrances. The final snapshot of the vaccine construct was preserved for subsequent modeling analyses. To evaluate its potential interaction with TLR4 (PDB ID: 4G8A) [30], docking studies were performed using the ClusPro 2.0 server (https://cluspro.org/login.php) [31]. After 500 ns MD simulation for relaxing the vaccine construct, a 100 ns MD simulation was assigned for vaccine: TLR4 complex.

simulations were conducted using the Desmond simulation software package developed by Schrödinger Inc [32]. Each MD run was performed with temperature set at 310 K and pressure maintained at 1 bar. The simulation was carried out using parameters from the OPLS3 (Optimized Potentials for Liquid Simulations, version 3) force field [33]. The calculation of extended electrostatic interactions was carried out applying the Particle Mesh Ewald (PME) approach [34], A cutoff radius of 9.0 Å was applied to treat Coulombic interactions. The system was solvated in an explicit TIP3P (three-site transferable intermolecular potential) water environment, enclosed within a cubic periodic box to maintain periodic boundary conditions [35]. To maintain system neutrality, Na^+ and Cl^- ions were incorporated as neutralizing ions. A minimum distance of 10.0 Å was maintained between the periodic boundary conditions and the nearest atoms of the vaccine: TLR4 complex. Pressure was controlled by means of the Martyna–Tuckerman–Klein chain scheme (Mark and Nilsson, 2001), while temperature was regulated using the Nosé–Hoover chain coupling scheme [36] throughout the MD simulations. Trajectory data were saved at intervals of 10 ps. Analysis of the MD results was performed using Visual Molecular Dynamics (VMD) [37], along with the Simulation Quality Analysis and Interaction Diagram modules integrated into the Desmond MD suite.

Immune response simulation of the multi-epitope vaccine candidate

To achieve an effective immune system response directed against DPP-4 cells, it is essential to gain insights into the immune properties of the developed vaccine using an immune simulation approach. Therefore, we evaluated the immune characteristics of the final multi-epitope vaccine by entering its sequence into the C-ImmSim 10.1 web server [38]. C-ImmSim is based on immunological principles that

model multiple components of the immune system, such as antigen processing and presentation to CTL and HTL, mechanisms such as intercellular signaling, maturation of B and T cells, development of memory cells, antigen-driven clonal selection, clonal deletion theory, antibody hypermutation, T-cell aging (replicative senescence), and induction of anergy in B and T lymphocytes, among others.

Results

T-cell epitope discovery and prioritization

A total of 28 CTL epitopes targeting the DPP-4 protein were identified through the NetCTL 1.2 server. The forecasted epitopes were subjected to a multi-step filtering procedure. In the initial step, epitopes that demonstrated binding to a minimum of three MHC class I supertypes were chosen. Subsequently, these selected epitopes were assessed for their Antigenicity, toxicity, and allergenicity through the utilization of VaxiJen v2.0, ToxinPred, and AllerTOP v2.0 servers, respectively. Ultimately, 6 CTL epitope (E1-E6) were chosen (Table 1). Additionally, a total of 33 HTL epitopes were predicted for DPP-4 the NetMHCII 2.3 server. Out of these epitopes, one specific epitope, denoted as D1, exhibited the ability to bind to a minimum of three MHC class II alleles while displaying both Antigenicity and the absence of toxicity and allergenicity (Table 2).

Table 1. Predicted CTL epitopes of DPP-4 protein.

TCL epitope	MHC class I alleles	Antigenicity	Toxicity	Allergenicity	Final decision
FTLDGNSFY	Supertype A26, A3, A1	Non-Antigen	Non-toxin	Probable allergen	-
WTGKEDIIY	Supertype A1, B62, A26	Non-Antigen	Non-toxin	Probable allergen	-
SSTAHQHIY	Supertype A1, B58, A3	Antigen	Non-toxin	Probable allergen	-
E1: RIAIWGWSY	Supertype A1, A3, A26, B58	Antigen	Non-toxin	Probable non-allergen	*
WISDHEYLY	Supertype A1, A26, B62	Non-Antigen	Non-toxin	Probable allergen	-
E2: YSVMDICDY	Supertype A1, A26, B58	Antigen	Non-toxin	Probable non-allergen	*

E3: YLYYISNEY	Supertype A1, A26, A3, B58	Antigen	Non-toxin	Probable non-allergen	*
FYSDESLQY	Supertype A1, A24, B62	Non-Antigen	Non-toxin	Probable allergen	-
E4: YVKQWRHSY	Supertype A1, A26, B8	Antigen	Non-toxin	Probable non-allergen	*
YEEEVFSAY	Supertype A1, A26, B39, B44, B62	Non-Antigen	Non-toxin	Probable non-allergen	-
STTGWVGRF	Supertype A1, A26, B58, B62	Non-Antigen	Non-toxin	Probable allergen	-
E5: GTADDNVHF	Supertype A1, A26, B58, B62	Antigen	Non-toxin	Probable non-allergen	*
E6: VSFSKEAKY	Supertype A1, A3, B58, B62	Antigen	Non-toxin	Probable non-allergen	*
ILNETKFWY	Supertype A1, A3, B58	Non-Antigen	Non-toxin	Probable non-allergen	-
ITAPASMLI	Supertype A1, A24, B58	Non-Antigen	Non-toxin	Probable non-allergen	-
KIEPNLPSY	Supertype A1, A3, A26, B62	Antigen	Non-toxin	Probable allergen	-
HIYTHMSHF	Supertype A3, A26, B58, B62	Antigen	Non-toxin	Probable allergen	-

YQMILPPHF	Supertype A24, B27, B58	Antigen	Non-toxin	Probable allergen	-
KQENNILVF	Supertype A24, B27, B39	Antigen	Non-toxin	Probable allergen	-
KIISNEEGY	Supertype A26, B58, B62	Antigen	Non-toxin	Probable allergen	-
FIILNETKF	Supertype A26, B8, B62	Non-Antigen	Non-toxin	Probable allergen	-
NILVFNAEY	Supertype A1, A26, B62	Non-Antigen	Non-toxin	Probable non-allergen	-
EGYRHICYF	Supertype A26, B8, B56	Non-Antigen	Non-toxin	Probable non-allergen	-
RVLEDNSAL	Supertype A2, B7	Antigen	Non-toxin	Probable non-allergen	-
YPKTVRVPY	Supertype B7, B8, B62	Antigen	Non-toxin	Probable allergen	-
RPSEPHFTL	Supertype B7, B8, B39	Antigen	Non-toxin	Probable allergen	-
YRHICYFQI	Supertype B7, B27, B39	Non-Antigen	Non-toxin	Probable allergen	-

YSFYSDESL	Supertype B39, B58, B62	Non-Antigen	Non-toxin	Probable allergen	-

HTL epitope	MHC class II alleles	Antigenicity	Toxicity	Allergenicity	IFN-γ – inducing	IL-4-inducing	Final decision
WKVLLGLLGAAALVT	DRB1_0101, DRB1_0402, DRB1_0403, DRB1_1001, DRB1_1201, DRB1_1602	Non-antigen	Non-Toxin	Probable non-allergen	Positive	Non-IL4-inducer	-
KVLLGLLGAAALVTI	DRB1_0101, DRB1_0402, DRB1_0403, DRB1_1001, DRB1_1602	Non-antigen	Non-Toxin	Probable non-allergen	Positive	Non-IL4-inducer	-
DTVFRLNWATYLAST	DRB1_0901, DRB1_01302, DRB3_0301, DRB1_0101, DRB1_1501, DRB1_ 0202	Antigen	Non-Toxin	Probable non-allergen	Negative	Non-IL4-inducer	-

PWKVLLGLLGAAALV	DRB1_0101, DRB1_0402, DRB1_1001, DRB1_1201, DRB1_1602	Non-antigen	Non-Toxin	Probable non-allergen	Positive	IL4-inducer	-
ADTVFRLNWATYLAS	DRB1_0101, DRB1_0901, DRB1_1302, DRB1_1501, DRB3_0202 DRB3_0301	Antigen	Non-Toxin	Probable non-allergen	Negative	Non-IL4-inducer	-
TVFRLNWATYLASTE	DRB1_0401, DRB1_0404, DRB1_0405, DRB1_1602, DRB3_0101, DRB3_0202	Antigen	Non-Toxin	Probable non-allergen	Negative	Non-IL4-inducer	-
VLLGLLGAAALVTII	DRB1_0101, DRB1_0402, DRB1_0403, DRB1_1001	Non-antigen	Non-Toxin	Probable non-allergen	Positive	Non-IL4-inducer	-
KADTVFRLNWATYLA	DRB1_0101, DRB1_0901, DRB1_1302, DRB3_0202, DRB3_0301	Antigen	Non-Toxin	Probable non-allergen	Negative	Non-IL4-inducer	-
TPWKVLLGLLGAAAL	DRB1_0901,	Non-antigen	Non-Toxin	Probable non-allergen	Positive	IL4-inducer	-

	DRB1_0101, DRB1_0901, DRB1_1602						
D1: LKNTYRLKLYSLRWI	DRB1_0103, DRB1_1201, DRB1_1501	Antigen	Non-Toxin	Probable non-allergen	Positive	IL4-inducer	*
GYQGDKIMHAINRRL	DRB1_0103, DRB1_0701, DRB1_1301	Non-antigen	Non-Toxin	Probable non-allergen	Negative	Non-IL4-inducer	-
YQGDKIMHAINRRLG	DRB1_0103, DRB1_0701, DRB1_1001, DRB1_1301	Non-antigen	Non-Toxin	Probable non-allergen	Negative	Non-IL4-inducer	-
QGDKIMHAINRRLGT	DRB1_0103, DRB1_0701, DRB1_1001, DRB1_1301	Non-antigen	Non-Toxin	Probable non-allergen	Negative	Non-IL4-inducer	-
GDKIMHAINRRLGTF	DRB1_0103, DRB1_0701, DRB1_1001, DRB1_1301, DRB1_1501	Non-antigen	Non-Toxin	Probable non-allergen	Negative	IL4-inducer	-
NPTVKFFVVNTDSLS	DRB1_0401, DRB1_0405, DRB3_0101, DRB3_0202	Non-antigen	Non-Toxin	Probable allergen	Negative	IL4-inducer	-
PTVKFFVVNTDSLSS	DRB1_0401,	Non-antigen	Non-Toxin	Probable allergen	Negative	IL4-inducer	-

	DRB1_0405, DRB3_0101, DRB3_0202						
TVKFFVVNTDSLSSV	DRB1_0401, DRB1_0404, DRB1_0405, DRB1_1602, DRB3_0101, DRB3_0202	Non-Antigen	Non-Toxin	Probable allergen	Negative	IL4-inducer	-
VKFFVVNTDSLSSVT	DRB1_0401, DRB1_0404, DRB1_0405, DRB1_1602, DRB3_0101, DRB3_0202	Antigen	Non-Toxin	Probable allergen	Negative	IL4-inducer	-
KFFVVNTDSLSSVTN	DRB1_0401, DRB1_0404, DRB1_0405, DRB1_1602, DRB3_0101, DRB3_0202	Antigen	Non-Toxin	Probable allergen	Negative	IL4-inducer	-
SEPHFTLDGNSFYKI	DRB1_0401, DRB1_0301, DRB3_0101	Antigen	Non-Toxin	Probable non-allergen	Negative	IL4-inducer	-
PHFTLDGNSFYKIIS	DRB1_0401, DRB1_0301, DRB3_0101	Antigen	Non-Toxin	Probable allergen	Negative	IL4-inducer	-

LDGNSFYKIISNEEG	DRB1_0401, DRB1_0405, DRB1_1602	Antigen	Non-Toxin	Probable allergen	Negative	IL4-inducer	-
GNSFYKIISNEEGYR	DRB1_0401, DRB1_0405, DRB1_1602	Antigen	Non-Toxin	Probable allergen	Negative	IL4-inducer	-
NSFYKIISNEEGYRH	DRB1_0401 DRB1_0405, DRB1_1602	Antigen	Non-Toxin	Probable allergen	Negative	IL4-inducer	-
DKIMHAINRRLGTFE	DRB1_0701, DRB1_0103, DRB1_1501, DRB1_1001, DRB1_1301	Antigen	Non-Toxin	Probable non-allergen	Negative	IL4-inducer	-
KIMHAINRRLGTFEV	DRB1_0701, DRB1_1001, DRB1_1301, DRB1_0103	Non-antigen	Non-Toxin	Probable non-allergen	Negative	IL4-inducer	-
RISLQWLRRIQNYSV	DRB1_0103, DRB1_0802, DRB1_01301 DRB1_1201, DRB1_1501 DRB1_0101	Non-antigen	Non-Toxin	Probable non-allergen	Negative	IL4-inducer	-
ISLQWLRRIQNYSVM	DRB1_0802, DRB1_0103, DRB1_1301,	Antigen	Non-Toxin	Probable non-allergen	Negative	Non-IL4-inducer	-

	DRB1_1201, DRB1_1501						
QKADTVFRLNWATYL	DRB1_0802, DRB4_0103, DRB1_1301, DRB1_1201, DRB1_1501	Antigen	Non-Toxin	Probable non-allergen	Negative	Non-IL4-inducer	-
VFRLNWATYLASTEN	DRB1_0901, DRB1_1302, DRB1_1501, DRB1_0202, DRB3-0301	Antigen	Non-Toxin	Probable non-allergen	Negative	Non-IL4-inducer	-
EEVFSAYSALWWSPN	DRB1_1001, DRB1_1602, DRB1_0402	Non-antigen	Non-Toxin	Probable non-allergen	Negative	Non-IL4-inducer	-
DGNSFYKIISNEEGY	DRB1_1602, DRB1_0405, DRB1_0401	Antigen	Non-Toxin	Probable allergen	Negative	IL4-inducer	-
EPHFTLDGNSFYKII	DRB1_0401, DRB3_0101, DRB1_0301	Antigen	Non-Toxin	Probable allergen	Negative	IL4-inducer	-

The interaction modes between the chosen CTL epitopes and their corresponding MHC class I have been demonstrated in Figures S1-S24. On the other hand, Figures S25-S27 illustrate the binding mode between HTL epitope and MHC class II (HLA-DRB1-0103, HLA-DRB1-1201, HLA-DRB1-1501) with the computed docking energy.

Construction of the vaccine and its secondary structure estimation

In the development of the diabetes vaccine, a combination of six CTL epitopes and one HTL epitope was employed. These epitopes were joined through AAY linker sequences connector, resulting in the creation of an 87 amino acid sequence. Additionally, an adjuvant sequence, spanning 130 amino acids (MAKLSTDELLDAFKEMTLLELSDFVKKFEETF EVTAAAPVAVAAAGAAPAGAAVEAAEEQSEF DVILEAAGDKKIGVIKVVREIVSGLGLKEAKDL

VDGAPKPLLEKVAKEAADEAKAKLEAAGATV TVK), was incorporated at the N-terminus of the construct using an EAAAK linker. The finalized vaccine model was comprised of 222 amino acids, as depicted in Figure 1A.

Antigenicity and prediction of molecular physicochemical parameters

The antigenicity properties of the vaccine sequence were estimated using the VaxiJen 2.0 server and followed by ANTIGENpro. The overall prediction for the constructed vaccine was performed by using VaxiJen 2.0 server was 0.6283 at a cutoff value of 0.5. Similarly, ANTIGENpro estimated the antigenicity probability at 0.7353. The molecular weight and theoretical isoelectric point of the final vaccine were calculated as 24.37 kDa and 5.15, respectively. Based on the predicted pI value, the vaccine construct exhibits an acidic nature. Its estimated half-life was 30 hours in mammalian reticulocytes (in vitro), over 20 hours in yeast, and more than 10 hours in E. coli (in vivo). The instability index value of 27.13 suggested that the vaccine construct is thermally stable (Rapin et al., 2010). The aliphatic index of the vaccine was 91.67, and its GRAVY score was reported to be 0.014.

Secondary structure prediction, tertiary structure modeling, refinement, and validation

The secondary structure profile of the multi-epitope vaccine was predicted using the Prabi server. The results indicated that the vaccine construct comprised 68.47% alpha-helices, 13.06% extended strands, and 18.47% random coils, as illustrated in Figure 1B. The five three-dimensional models of the vaccine construct were produced by I-TASSER, leveraging six threading templates (PDB hits: 1dd4 chain A, 1rqu chain A, 7ou3 chain A, 2ftc, 1dd3 chain A, 8dt0 chain A). The calculated C-scores for models 1–5 was −3.2, −3.43, −3.74, −4.17, and −3.72, respectively. Since C-scores generally range from −5 to 2, higher values indicate greater confidence in the predicted model. (Garnier, 1998). In the subsequent phase, the ProTSAV server was employed to assess the accuracy of each predicted model (Figures 2A-E). Model 1, selected based on its ProTSAV overall score, underwent additional refinement using the GalaxyRefine2 web server, and its ProTSAV overall score was re-evaluated (Figure 2F).

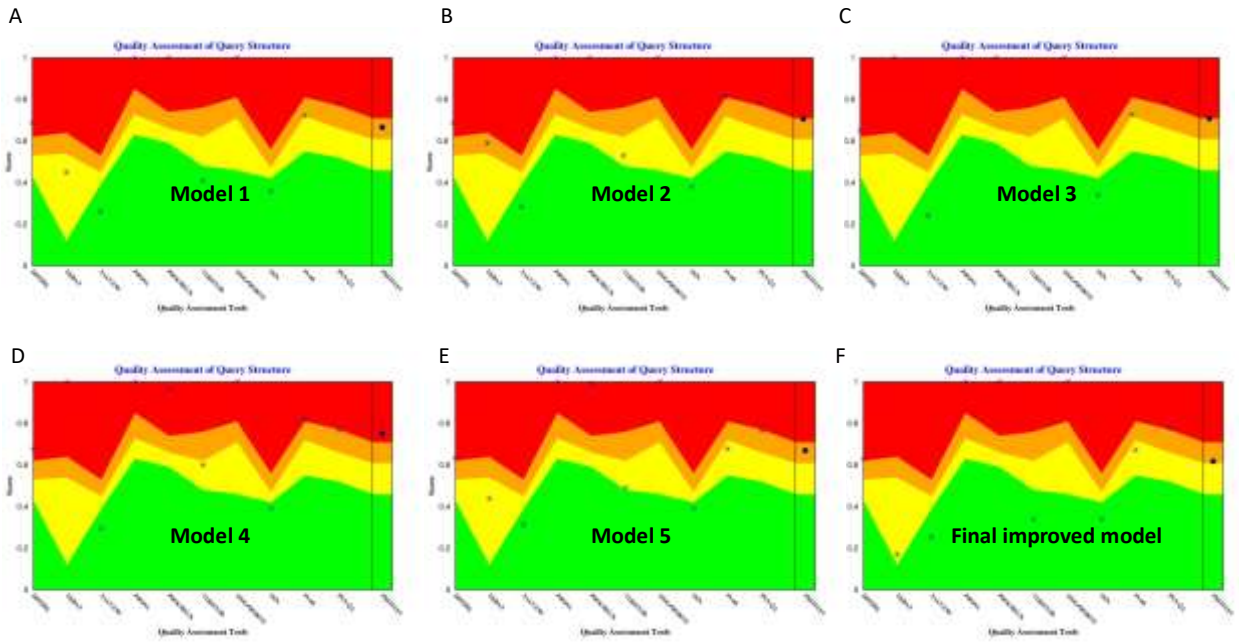

Figure 2: ProTSAV quality assessment of input vaccine models; (A) 1, (B) 2, (C) 3, (D) 4, (E) 5, and (F) further refined model. Green region indicates the input structure to be in 0–2 Å rmsd, yellow region 2–5 Å rmsd, orange region 5–8 Å rmsd and red region indicates structures beyond 8 Å rmsd. The blue colored asterisk symbol represents quality assessment score by individual module and blue colored round symbol represents overall score by ProTSAV.

B-cell epitope prediction

A set of three 7-mer linear B-cell epitopes, consisting of LELSDFV, SEFDVIL, KIGVIKVVREIVSGLGL, KPLLEKV, YSVMDICDY, YYLYYISN, and YRLKLYSLR were predicted by the BCPREDS. In addition, the ElliPro server predicted five discontinuous B-cell epitopes within the tertiary structure of the vaccine construct (Figure 3). For the discontinuous B-cell epitopes, the lowest and highest scores were 0.555 and 0.837, respectively (Table 3).

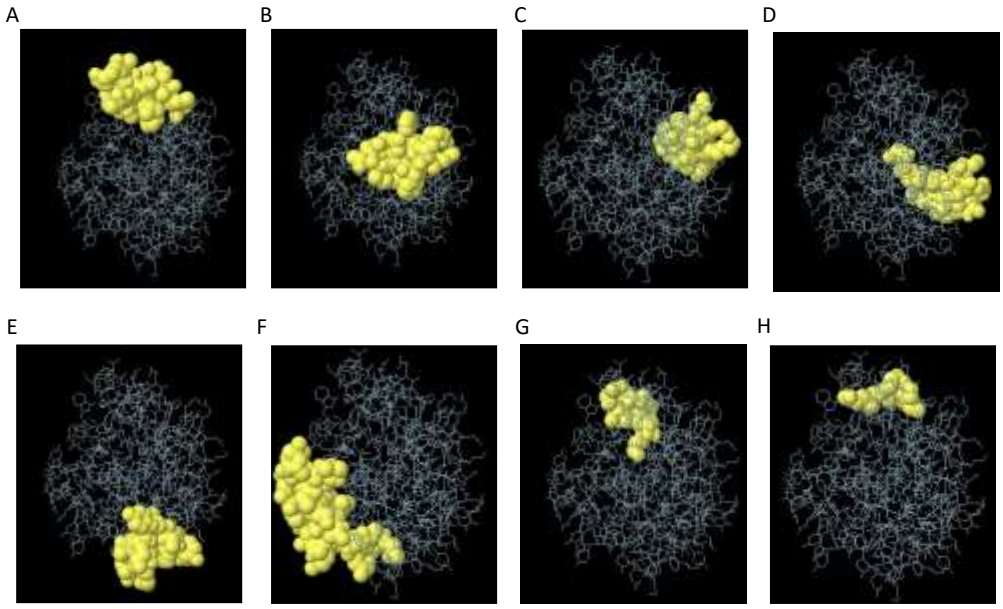

Figure 3: (A–H) The discontinuous B-cell epitopes on the vaccine construct's 3D structure. The gray sticks and the yellow surface show the vaccine construct and discontinuous B-cell epitopes, respectively

Table 3: Discontinuous B-cell epitopes identified through ElliPro analysis

Start	End	Peptide	Number of residues	Score
1	17	MAKLSTDELLDAFKEMT	17	0.837
27	39	KFEETFEVTAAAP	13	0.747
114	127	DEAKAKLEAAGATV	14	0.731
64	84	EAAGDKKIGVIKVVREI	17	0.684
197	211	SFSKEAKYAAYLKNT	15	0.646
167	190	EYAAYYVKQWRHSYAAYGTADDNV	24	0.622
130	136	KEAAAKR	7	0.588
58	61	EEQS	4	0.555

Predicted interaction of the vaccine construct with TLR4

Docking studies between the vaccine construct and TLR4 were performed using the ClusPro 2.0 server. The server generated 29 clusters, The server produced 29 clusters, which were then ranked according to their energy values. The cluster exhibiting the minimum binding energy, registering at -1041.1, was identified as the optimal complex (Figure 4). Notably, Arg220 of the vaccine engaged in salt-bridge interactions with TLR4 residues Glu605A and Glu603A. Additionally, a salt-bridge was established between Arg177 from the vaccine and Glu144C from TLR4. Further stabilization of the vaccine: TLR4 complex was achieved via the formation of three hydrogen bonds.

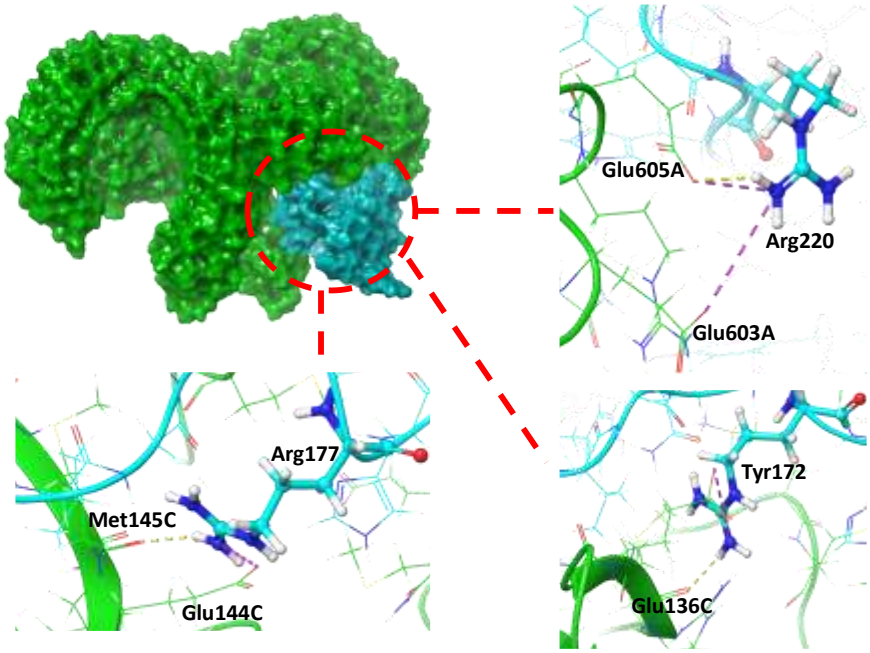

Figure 4: Molecular docking of vaccine construct with TLR4 as an immune receptor. H-bonds, salt-bridge, and π-cation interactions are shown as yellow, purple and green dashed lines, respectively

Molecular dynamics evaluation of the vaccine–TLR4 complex

The MD simulation spanned a robust 100 nanosecond timescale, during which we meticulously analyzed a variety of critical intermolecular interactions. We generated insightful plots for Root Mean Square Deviation (RMSD), Root Mean Square Fluctuation (RMSF), and Radius of gyration (Rg) to assess the dynamic flexibility and overall stability of the vaccine-receptor complex, as depicted in Figure 5. Our MD results provided valuable insights into the nature of interactions within the complex. Notably, hydrogen bonding emerged as the predominant non-covalent interaction between the vaccine construct and TLR4, exhibiting an average value of 16.67 H-bonds (Figure 5A). Meanwhile, the average count of salt-bridge interactions between the two proteins was determined to be 2.76, highlighting their significance in the binding process. In contrast, π-π stacking and π-cation interactions exhibited a comparatively minor contribution to the overall binding phenomenon (Figure 5A). The RMSD plot exhibited significant results highlighting the stability of the vaccine: TLR4 complex (Figure 5B). Our data unveiled that the vaccine exhibited greater movement and flexibility relative to the TLR4 receptor. However, the RMSD values for the vaccine: TLR4 complex were comparatively lower. RMSF shows the movement and flexibility of each residue during the MD simulation. Figure 5C illustrates the distribution of RMSD values for the vaccine, TLR4, and the vaccine: TLR4 complex throughout the MD simulations. Upon Figure 5D, the regions of heightened flexibility were primarily concentrated at the loop area and N-terminal of the vaccine. The Radius of Gyration (Rg) serves as an indicator of how tightly the complex is packed. A stable complex should show limited movement or change in the positions of TLR4 and vaccine residues throughout the simulation. Notably, the Rg plot in Figure 5E revealed minimal deviation for both proteins from 20 to 100 ns in the simulation, underscoring the stability of the complex. After clustering the MD trajectories, we performed an in-depth analysis of the interactions between vaccine and TLR4 residues, with the results summarized in Table 4.

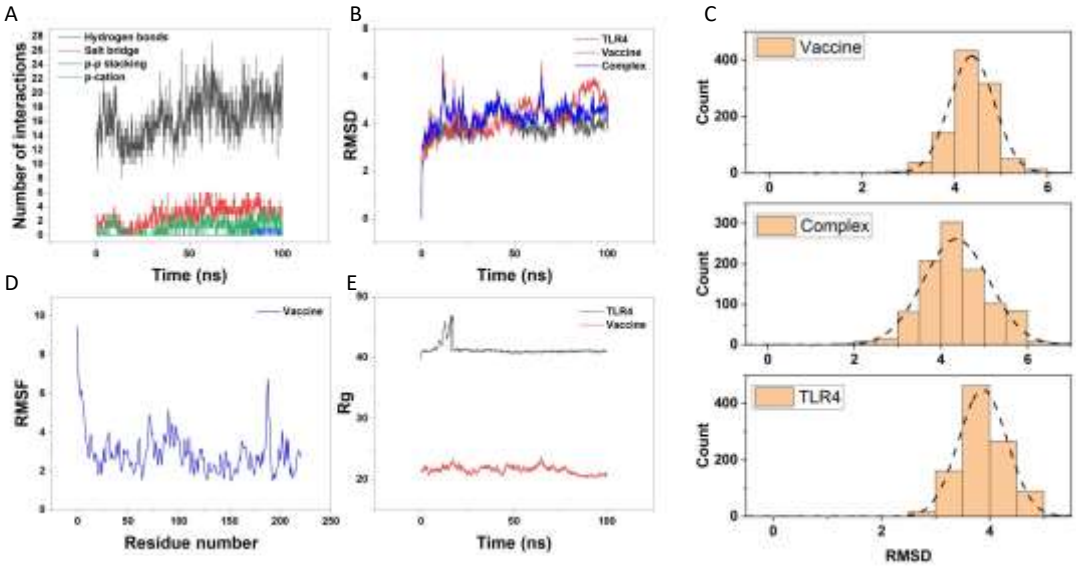

Figure 5: Molecular dynamics simulation trajectory plot of final vaccine construct with TLR4. A) Number of interactions between the vaccine and TLR4. B) RMSD of vaccine, TLR4, and vaccine:TLR4 complex. C) The distribution of RMSD values. D) RMSF of vaccine. E) Rg of vaccine and TLR4.

Table 4: The interaction between vaccine and TLR4 residues followed by cluster analysis during MD simulation.

Vaccine residue	TLR4 residue and chain	Distance (Å)	Type of interaction
Thr126	Asn35, A	2	Hydrogen bond
Arg177	Glu42, A	2.2	Hydrogen bond
Ser179	Asn44, A	1.8	Hydrogen bond
Tyr168	Glu578, A	1.8	Hydrogen bond
Glu92	Arg598, A	1.9	Hydrogen bond
Tyr 217	Gln616, A	2.1	Hydrogen bond
Lys 203	Glu485, B	2.1	Hydrogen bond
Val 190	Gln19, C	1.7	Hydrogen bond
Asp 188	Lys20, C	2	Hydrogen bond

His 191	Tyr36, C	2.1	Hydrogen bond
Trp 176	Cys37, C	2.1	Hydrogen bond
Asn 189	Asp38, C	2.3	Hydrogen bond
Asn 189	Lys39, C	2.2	Hydrogen bond
Asp 187	Lys39, C	2.3	Hydrogen bond
Asp 188	Lys39, C	2.5	Hydrogen bond
Asn 189	Gln41, C	1.9	Hydrogen bond
Tyr 207	Leu87, C	1.8	Hydrogen bond
Ala 170	Glh136, C	1.5	Hydrogen bond
Glu 92	Arg598, C	1.9	Salt-bridge
Lys 203	Glu485, C	2.1	Salt-bridge
Asp 187	Lys39, C	2.3	Salt-bridge
Tyr 207	Tyr79, C	2.4	π -π stacking

In total, the analysis revealed the formation of eighteen hydrogen bonds, three salt-bridges and one π -π stacking between the vaccine and the receptor (Table 4).

Immune simulation of vaccine construct

The results obtained from the in-silico C-ImmSim immune simulation align closely with actual immune responses observed in the real world. This alignment is substantiated by a notable increase in the generation of secondary responses (Figure 6A-I). The primary immune response stood out due to a significant presence of immunoglobulin M (IgM). Subsequent immunizations, encompassing both secondary and tertiary responses, exhibited prominent elevations in antibody levels, encompassing IgG1 + IgG2, IgM, and IgG + IgM. This trend was accompanied by a concurrent decrease in antigen concentration, as illustrated in Figure 6A and 6F. In our present study, we noted a significant increase in the lymphocyte population and elevated production of IFN-γ and IL-2 in the immune simulation for the vaccine, as illustrated in Figure 6B. Moreover, the vaccine construct triggered the proliferation of B-cell populations following each subsequent injection, as depicted in Figure 6C. Simulation results reveal the establishment of immune memory in the vicinity of the intermediate period, as illustrated in Figure 6D. Additionally, a significantly heightened response is evident in both helper and cytotoxic T-cell populations, occurring concurrently with the development of memory cells, as depicted in Figures 6D, 6E, 6G, and 6H. Following

the administration of the vaccine, a noteworthy increase in NK cell counts is observed, and this elevated level is sustained throughout the simulation period, as indicated in Figure 6I.

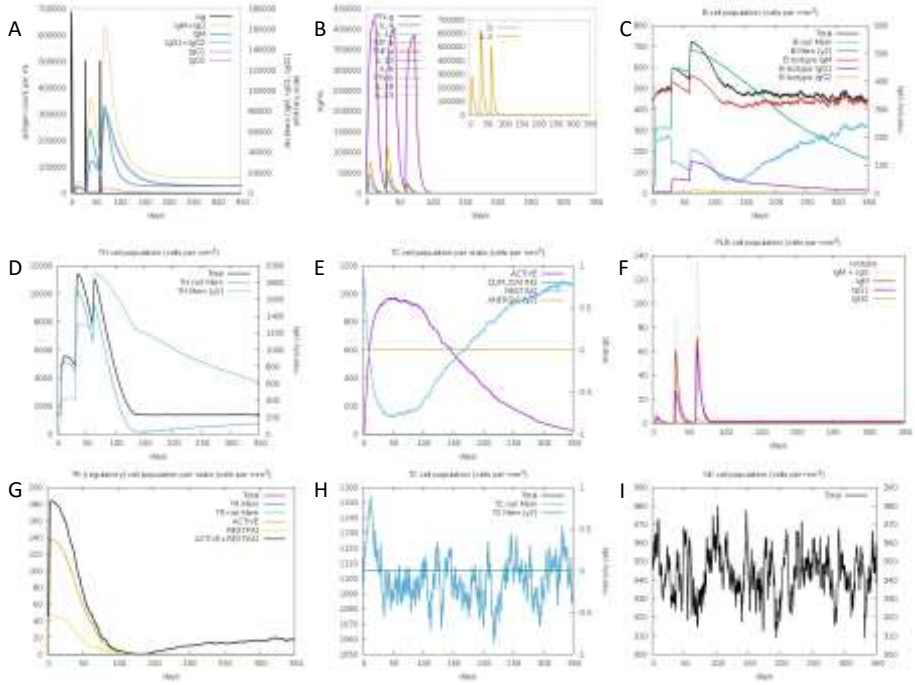

Figure 6: Immune simulation of the final construct vaccine after three injections. (A) The frequency of different Immunoglobulin and immunocomplexes production in response to antigen injections (black). Various subclasses are presented as colored peaks. (B) Various cytokine and interleukins. (C) The prediction of computed B-cell amounts. (D) The prediction of T-helper, (E) T-cytotoxic cell amounts per state, (F) various IgG subclasses, (G) CD4 T-regulatory lymphocytes count showing total/memory/per entity-state counts, (H) CD8 T-cytotoxic lymphocytes count showing total and memory populations, and (I) NK cell populations after three vaccine injections.

Discussion

Enduring as a significant global health challenge, DM, impacts individuals across diverse ages, ethnicities, and backgrounds. This influence is particularly pronounced among those with a notable family history of diabetes and a myriad of environmental factors [39]. In this study, a peptide-based vaccine against DPP4 was designed with the aim of elevating GLP-1 levels and enhancing insulin sensitivity. Prior research has conveyed that the incretin hormone GLP-1 goes beyond merely stimulating glucose-induced insulin secretion. It plays a pivotal role in enhancing glycogen synthesis, glucose oxidation, and utilization in key metabolic tissues such as skeletal muscle, liver, and adipose tissue [40-42]. Additionally, noteworthy findings in mice deficient in the gene encoding DPP4 revealed that heightened GLP-1 levels effectively improved insulin sensitivity and mitigated hyperinsulinemia induced by a high-fat diet [43]. In addition, there are reports suggesting that GLP-1 might exert its influence on glucose control independently of insulin secretion, operating through the activation of peripheral sensors associated with improved glucose disposal [44].

While oral DPP4 inhibitors prove to be both safe and efficacious in treating T2DM, their daily administration may result in peak variations throughout the day [10], posing not only potential fluctuations in effectiveness but also imposing an economic burden on the patient. The designed vaccine construct exhibited favorable antigenicity and was predicted to be non-allergenic. This suggests its potential to elicit robust immune responses without

inducing adverse allergic reactions. The theoretical isoelectric point (pI) of the vaccine was determined to be 5.15, indicating its acidic character. With a molecular weight of 24.37 kDa, the vaccine falls within a desirable range, as proteins under 110 kDa are generally more amenable to efficient purification processes [45]. The vaccine construct displayed a high α-helical content (68.47%), with an instability index calculated at 27.13. Since this value is below the threshold of 40, the construct is classified as a stable protein. [19].

In 2021, Gharbavi et al. [46] developed a vaccine construct incorporating three proteins: IL-13Rα2, TNC, and PTPRZ-1 [47]. Our vaccine demonstrated a prolonged half-life of 30 hours in mammalian reticulocytes, surpassing the 1.1-hour half-life observed in the constructs designed by Gharbavi et al. [47]. This extended half-life suggests that our vaccine remains exposed to the immune system for a more extended duration compared to the formulations by Gharbavi et al. The aliphatic index of our vaccine was computed at 91.67, surpassing those of vaccines designed by Gharbavi et al. [47], Sanami et al. [46], and Kumar et al. [48]. This higher aliphatic index indicates the thermostability of our vaccine.

After predicting the three-dimensional structure of the vaccine, we implemented a refinement process aimed at improving its quality and aligning it more closely with its native conformation. A comprehensive evaluation of the model's quality was then conducted, affirming the high standard and reliability of our vaccine model. Molecular docking analysis revealed a strong binding interaction between the vaccine construct and TLR4. Following this, the docked vaccine–TLR4 complex was further investigated through MD simulation to assess the stability of the construct. The simulation data underscored hydrogen bonding as a key stabilizing interaction between the vaccine and TLR4. The RMSD plot, constructed for the proposed vaccine and TLR4, indicated the stability of vaccine/TLR4 complex. Additionally, RMSF analysis showed that the vaccine construct exhibited low flexibility, especially in regions engaged in extensive interactions with TLR4. Rg calculations indicated that both TLR4 and the vaccine maintained structural stability throughout the MD simulation. The in-silico simulation of the immune response demonstrated a progressive enhancement in immune reactions upon recurrent exposures to the antigen. The increased activity of B and T cells, coupled with the prolonged memory of B cells spanning several months, signifies the activation of humoral immunity. This aspect is crucial for augmenting and enhancing the overall immune response. Elevated production of IFN-γ and IL-2 during repeated antigen exposure suggests a cell-mediated immune response. Given that the cytokine IFN-γ plays a role within the process of B-cell division and immunoglobulin isotype switching, as referenced in studies [49,50], it also facilitates the support of a humoral response.

Conclusion

This study successfully designed a peptide-based vaccine targeting DPP-4 to manage diabetes mellitus, a significant global health challenge. The vaccine design involved a combination of CTL and HTL epitopes and an adjuvant sequence, aiming to elevate GLP-1 levels and increase insulin sensitivity. The vaccine demonstrated high antigenicity, stability, and a favorable interaction with TLR4. The MD study indicated the structural immune simulation outcomes showed an enhanced immune response, highlighting the vaccine's potential in activating both humoral and cell-mediated immunity. This innovative approach to diabetes management could offer a significant advance over current treatment modalities, potentially reducing the need for daily medication and easing the economic burden on patients.

Declarations

Conflict of Interest

The author declares no conflict of interest related to the publication of this article.

Acknowledgements

The author extends sincere appreciation to Institute of Medical Science, University of Toronto, Canada for their valuable support and contributions to this research.

Consent for Publication

The author confirms that the final version of the manuscript has been reviewed and approved for publication.

Funding/Support

None.

Authors' Contributions

FA and SM was responsible for conceptualization, review, data collection, analysis, writing, and manuscript preparation.

Ethical Approval

As this study is a review article, it does not involve human or animal subjects and therefore does not require ethical approval or informed consent.

References

1. Zimmet P, Alberti KG, Magliano DJ, Bennett PH. Diabetes mellitus statistics on prevalence and mortality: facts and fallacies. Nat Rev Endocrinol. 2016;12(10):616–22. doi:10.1038/nrendo.2016.105.
2. Tuomi T, Santoro N, Caprio S, Cai M, Weng J, Groop L. The many faces of diabetes: a disease with increasing heterogeneity. Lancet. 2014;383(9922):1084–94.
3. Yousef CC, Thomas A, Al Matar M, Ghandoura L, Aldossary I, Almuhanna SM, et al. Liraglutide effects on glycemic control and weight in patients with type 2 diabetes mellitus: a real-world, observational study and brief narrative review. Diabetes Res Clin Pract. 2021;177:108871. doi:10.1016/j.diabres.2021.108871.
4. Olokoba AB, Obateru OA, Olokoba LB. Type 2 diabetes mellitus: a review of current trends. Oman Med J. 2012;27(4):269. doi:10.5001/omj.2012.68.
5. Khursheed R, Singh SK, Wadhwa S, Kapoor B, Gulati M, Kumar R, et al. Treatment strategies against diabetes: success so far and challenges ahead. Eur J Pharmacol. 2019;862:172625. doi:10.1016/j.ejphar.2019.172625.
6. Forouhi NG, Wareham NJ. Epidemiology of diabetes. Medicine (Abingdon). 2010;38(11):602–6.
7. Nauck MA, Meier JJ. Incretin hormones: their role in health and disease. Diabetes Obes Metab. 2018;20(Suppl 1):5–21. doi:10.1111/dom.13129.
8. Bellary S, Kyrou I, Brown JE, Bailey CJ. Type 2 diabetes mellitus in older adults: clinical considerations and management. Nat Rev Endocrinol. 2021;17(9):534–48.
9. Gallwitz B. Clinical use of DPP-4 inhibitors. Front Endocrinol. 2019;10:389.
10. Sesti G, Avogaro A, Belcastro S, Bonora BM, Croci M, Daniele G, et al. Ten years of experience with DPP-4 inhibitors for the treatment of type 2 diabetes mellitus. Acta Diabetol. 2019;56(6):605–17. doi:10.1007/s00592-018-1271-3.
11. Pang Z, Nakagami H, Osako MK, Koriyama H, Nakagami F, Tomioka H, et al. Therapeutic vaccine against DPP4 improves glucose metabolism in mice. Proc Natl Acad Sci USA. 2014;111(13):E1256–63.
12. Chen X, Qiu Z, Yang S, Ding D, Chen F, Zhou Y, et al. Effectiveness and safety of a therapeutic vaccine against angiotensin II receptor type 1 in hypertensive animals. Hypertension. 2013;61(2):408–16. doi:10.1161/HYPERTENSIONAHA.112.201020.
13. Burnier M. Long-term compliance with antihypertensive therapy: another facet of chronotherapeutics in hypertension. Blood Press Monit. 2000;5(Suppl 1):S31–4.
14. Carel JC, Boitard C, Eisenbarth G, Bach JF, Bougnères PF. Cyclosporine delays but does not prevent clinical onset in glucose intolerant pre-type 1 diabetic children. J Autoimmun. 1996;9(6):739–45.
15. Petrovsky N, Silva D, Schatz DA. Vaccine therapies for the prevention of type 1 diabetes mellitus. Paediatr Drugs. 2003;5(9):575–82. doi:10.2165/00148581-200305090-00001.
16. Ghandadi M. An immunoinformatic strategy to develop new Mycobacterium tuberculosis multi-epitope vaccine. Int J Pept Res Ther. 2022;28(3):1–14.
17. Doytchinova IA, Flower DR. VaxiJen: a server for prediction of protective antigens, tumour antigens and subunit vaccines. BMC Bioinformatics. 2007;8:4.
18. Dimitrov I, Bangov I, Flower DR, Doytchinova I. AllerTOP v.2—a server for in silico prediction of allergens. J Mol Model. 2014;20(6):2278. doi:10.1007/s00894-014-2278-5.
19. Magnan CN, Zeller M, Kayala MA, Vigil A, Randall A, Felgner PL, et al. High-throughput prediction of protein antigenicity using protein microarray data. Bioinformatics. 2010;26(23):2936–43. doi:10.1093/bioinformatics/btq551.
20. Gasteiger E, Hoogland C, Gattiker A, Duvaud SE, Wilkins MR, Appel RD, et al. Protein identification and analysis tools on the ExPASy server. In: Walker JM, editor. The Proteomics Protocols Handbook. Totowa: Humana Press; 2005. p. 571–607.
21. Garnier J. GOR secondary structure prediction method version IV. In: Doolittle RF, editor. Methods Enzymol. 1998;266:540–53. doi:10.1016/S0076-6879(96)66034-0.
22. Roy A, Kucukural A, Zhang Y. I-TASSER: a unified platform for automated protein structure and function prediction. Nat Protoc. 2010;5(4):725–38.

23. Singh A, Kaushik R, Mishra A, Shanker A, Jayaram B. ProTSAV: a protein tertiary structure analysis and validation server. Biochim Biophys Acta Proteins Proteomics. 2016;1864(1):11–9.
24. Lee GR, Won J, Heo L, Seok C. GalaxyRefine2: simultaneous refinement of inaccurate local regions and overall protein structure. Nucleic Acids Res. 2019;47(W1):W451–5. doi:10.1093/nar/gkz288.
25. Khan M, Khan S, Ali A, Akbar H, Sayaf A, Khan A, et al. Immunoinformatics approaches to explore Helicobacter pylori proteome (virulence factors) to design B and T cell multi-epitope subunit vaccine. Sci Rep. 2019;9:1–13.
26. Saha S, Raghava GPS. BcePred: prediction of continuous B-cell epitopes in antigenic sequences using physico-chemical properties. In: Proc Int Conf Artif Immune Syst. Springer; 2004. p. 197–204.
27. Chen J, Liu H, Yang J, Chou KC. Prediction of linear B-cell epitopes using amino acid pair antigenicity scale. Amino Acids. 2007;33(3):423–8.
28. Ponomarenko J, Bui HH, Li W, Fusseder N, Bourne PE, Sette A, et al. ElliPro: a new structure-based tool for the prediction of antibody epitopes. BMC Bioinformatics. 2008;9:514.
29. Laxmi D, Priyadarshy S. HyperChem 6.03. Biotechnol Softw Internet Rep. 2002;3(1):5–9.
30. Trott O, Olson AJ. AutoDock Vina: improving the speed and accuracy of docking with a new scoring function, efficient optimization, and multithreading. J Comput Chem. 2010;31(2):455–61.
31. Ohto U, Yamakawa N, Akashi-Takamura S, Miyake K, Shimizu T. Structural analyses of human Toll-like receptor 4 polymorphisms D299G and T399I. J Biol Chem. 2012;287(48):40611–7.
32. Desta IT, Porter KA, Xia B, Kozakov D, Vajda S. Performance and its limits in rigid body protein–protein docking. Structure. 2020;28(9):1071–81.e3. doi:10.1016/j.str.2020.06.006.
33. Schrödinger Release 3. Desmond Molecular Dynamics System. New York: D.E. Shaw Research; 2017.
34. Banks JL, Beard HS, Cao Y, Cho AE, Damm W, Farid R, et al. Integrated modeling program, applied chemical theory (IMPACT). J Comput Chem. 2005;26(16):1752–80. doi:10.1002/jcc.20292.
35. Toukmaji AY, Board JA Jr. Ewald summation techniques in perspective: a survey. Comput Phys Commun. 1996;95(2–3):73–92.
36. Martyna GJ, Tuckerman ME, Tobias DJ, Klein ML. Explicit reversible integrators for extended systems dynamics. Mol Phys. 1996;87(5):1117–57.
37. Martyna GJ, Klein ML, Tuckerman M. Nosé–Hoover chains: the canonical ensemble via continuous dynamics. J Chem Phys. 1992;97(4):2635–43.
38. Humphrey W, Dalke A, Schulten K. VMD: visual molecular dynamics. J Mol Graph. 1996;14(1):33–8.
39. Ikai A. Thermostability and aliphatic index of globular proteins. J Biochem. 1980;88(6):1895–8.
40. Chellappan DK, Bhandare RR, Shaik AB, Prasad K, Suhaimi NAA, Yap WS, et al. Vaccine for diabetes—where do we stand? Int J Mol Sci. 2022;23(16):9470. doi:10.3390/ijms23169470.
41. Gedulin BR, Nikoulina SE, Smith PA, Gedulin G, Nielsen LL, Baron AD, et al. Exenatide (exendin-4) improves insulin sensitivity and β-cell mass in insulin-resistant obese fa/fa Zucker rats independent of glycemia and body weight. Endocrinology. 2005;146(4):2069–76. doi:10.1210/en.2004-1349.
42. Sandhu H, Wiesenthal SR, MacDonald PE, McCall RH, Tchipashvili V, Rashid S, et al. Glucagon-like peptide 1 increases insulin sensitivity in depancreatized dogs. Diabetes. 1999;48(5):1045–53. doi:10.2337/diabetes.48.5.1045.
43. Villanueva-Penacarrillo M, Alcantara A, Clemente F, Delgado E, Valverde I. Potent glycogenic effect of GLP-1 (7–36) amide in rat skeletal muscle. Diabetologia. 1994;37(11):1163–6.
44. Conarello SL, Li Z, Ronan J, Roy RS, Zhu L, Jiang G, et al. Mice lacking dipeptidyl peptidase IV are protected against obesity and insulin resistance. Proc Natl Acad Sci USA. 2003;100(11):6825–30.
45. Drucker DJ. The biology of incretin hormones. Cell Metab. 2006;3(3):153–65.
46. Gharbavi M, Danafar H, Amani J, Sharafi A. Immuno-informatics analysis and expression of a novel multi-domain antigen as a vaccine candidate against glioblastoma. Int Immunopharmacol. 2021;91:107265. doi:10.1016/j.intimp.2020.107265.
47. Barh D, Barve N, Gupta K, Chandra S, Jain N, Tiwari S, et al. Exoproteome and secretome derived broad spectrum novel drug and vaccine candidates in Vibrio cholerae targeted by Piper betel derived compounds. PLoS One. 2013;8(1):e52773. doi:10.1371/journal.pone.0052773.
48. Sanami S, Azadegan-Dehkordi F, Rafieian-Kopaei M, Salehi M, Ghasemi-Dehnoo M, Mahooti M, et al. Design of a multi-epitope vaccine against cervical cancer using

immunoinformatics approaches. Sci Rep. 2021;11(1):12397.
49. Fang D, Cui K, Mao K, Hu G, Li R, Zheng M, et al. Transient T-bet expression functionally specifies a distinct T follicular helper subset. J Exp Med. 2018;215(11):2705–14. doi:10.1084/jem.20180927.
50. Kumar S, Shuaib M, Prajapati KS, Singh AK, Choudhary P, Singh S, et al. A candidate triple-negative breast cancer vaccine design by targeting clinically relevant cell surface markers: an integrated immuno and bioinformatics approach. 3 Biotech. 2022;12(3):72.